Asociación Argentina
de Mecánica Computacional

Mecánica Computacional Vol XXVII, págs. 1619-1636 (artículo completo)
Alberto Cardona, Mario Storti, Carlos Zuppa. (Eds.)
San Luis, Argentina, 10-13 Noviembre 2008

TURBULENT SCALAR TRANSPORT MECHANISM AND VELOCITY-TEMPERATURE NATURAL DISSIMILARITY IN A TURBULENT PLANE COUETTE FLOW

Hugo D. Pasinato

Dpto. de Ing. Química,
RAC, Universidad Tecnológica Nacional,
Plaza Huincul, Neuquén, hpasinato@uacf.utn.edu.ar,
http://www.uacf.utn.edu.ar

Keywords: Velocity and temperature dissimilarity; Direct Numerical Simulation.

Abstract. The direct numerical simulation, DNS, of a fully developed turbulent plane Couette flow with heat transfer has been performed. The main goals of the present work is to analyse natural dissimilarity, and axial momentum and thermal energy turbulent transport mechanism in this kind of turbulence. It has been chosen a low Reynolds number equal to 1,300 as a function of half the walls distance and half the velocity of the moving wall. This Reynolds gives a Reynolds number as a function of half walls distance and friction velocity of about 84. The energy equation was solved for a molecular Prandtl number equal 1, and with isothermal boundary conditions at both walls. For instance, the streamwise velocity and temperature fields were solved with the same kind of boundary conditions, in order to have the same direction of momentum and thermal turbulent fluxes. Buoyancy effects were neglected, thus the temperature was considered as a passive scalar.

The main results of this work show that axial velocity and temperature fluctuations have the same kind of natural dissimilarity present in turbulent channel flow. While natural de-correlation between axial velocity and temperature fluctuations starts in the very near-wall region due to the most energetic events there, the contribution of these events to the total natural dissimilarity is less than fifty percent in the whole flow.

Analysis of longitudinal velocity and temperature fluctuations in the frequency domain, using spectral density functions, shows that the main cause of natural dissimilarity is the shift toward higher frequencies of temperature fluctuations in comparison to those belong to axial velocity, in the viscous, buffer, and beginning of the logarithmic region. Based on the spectra of pressure fluctuations and wall normal fluctuations, it is clear that wall normal velocity plays an important role in the natural dissimilarity of streamwise velocity and temperature fluctuation fields.

1 INTRODUCTION

Turbulent heat transfer is a phenomenon of fundamental importance in science and technology. In many situations, however, its prediction in applied problems uses the Reynolds analogy or similarity between momentum and heat transfer, which is not universal. (In this context, similarity between momentum and heat transfer means mean flow and fluctuations similarity, between axial velocity and temperature). For this reason velocity and temperature similarity and dissimilarity in turbulent flows has been extensively studied experimentally, and numerically, for different situations. The correlation between these fluctuations in wall bounded turbulent flow has been intensively investigated in the last three decades, first experimentally and then numerically. And as it has been shown in the literature with experimental works (Bremhorst and Bullock 1970; Orlando, Moffat, and Kays, 1974; Zaric 1975; Fulachier and Dumas, 1976; Hishida and Nagano 1979; Iritani, Kasagi, and Hirata 1985; Antonia, Krishnamoorthy, and Fulachier 1988), and numerical works (Kim and Min, 1989; Kasagi, Tomita, and Kuroda, 1992; Kawamura, Abe, and Matsuo 1999; Na, Papavassiliou, and Hanratty 1999; Na, and Hanratty 2000; Kong, Choi, and Lee 2000, and Kong, Choi, and Lee 2001), the similarity between the axial velocity and temperature fields, is very strong in the viscous and buffer region of a turbulent boundary layer. In those cases, for instance, with similar boundary conditions for the axial momentum and thermal fields, the normal fluxes of axial momentum and heat have the same direction, and the similarity is stronger.

A special and interesting study case is without doubt developed plane turbulent Couette flow. Plane Couette turbulent flow is one of the canonical flow cases. In comparison with zero pressure gradient boundary layers and pressure driven channel flow, plane Couette flow has the unique feature of combining the parallel flow property with zero pressure gradient. For this reason this kind of turbulent flow is an excellent flow case for axial velocity and temperature similarity and dissimilarity study. For instance heat transfer in plane Couette flow with isothermal walls has the same kind of axial velocity and temperature boundary conditions, while the axial momentum and thermal turbulent fluxes have also the same direction. All these features make turbulent plane Couette flow with isothermal walls a very special experiment for velocity and temperature similarity-dissimilarity study.

Developed plane turbulent Couette flow, however, has proved to be more difficult to simulate numerically than other canonical flows like as, for example, developed channel turbulent flow. The difficulty is mainly due the existence of very large streamwise structures in the center region of the flow. In the last decade, however, there have been enough research that gives some confidence using this kind of turbulence in numerical experiment for heat transfer study (Komminaho, Lundbladh, and Johansson, 1996; Tillmark and Alfredsson, 1992; Debusschere and Rutland, 2000; Bech et al, 1995).

Developed turbulent Couette flow has some similar characteristics to fully developed turbulent channel flow. But these flows present also some important differences. For example, both flows have similar near-wall structure (Aydin and Leutheusser, 1991), however the Reynolds stresses distribution is different. In turbulent channel flow the Reynolds stresses are maximum near the wall and then approach zero at the center line. In Couette flow, in contrast, Reynolds stresses increase from the wall to a maximum at the center line. The turbulent kinetic energy production, on the other hand, in a Couette flow has a finite value through the whole flow, while in turbulent channel flow the production of turbulence goes to zero at the centerline of the channel. For these reasons it seems appropriate to perform numerical experiments with heat transfer

in this kind of turbulence, with the objective to see if natural dissimilarity of axial velocity and temperature fluctuations present the same behavior as in turbulent channel flows.

In a previous work (Pasinato, 2007) the natural dissimilarity in a fully developed turbulent channel flow was studied using DNS. The main results of this work was that natural dissimilarity occurs basically due to the background turbulence. Or in other words, that the most energetic events in the wall layer, as a consequence of sweeping and ejection motions, do not contribute significantly in a direct way to the de-correlation between axial velocity and temperature afar from the wall. For a developed turbulent channel flow the natural dissimilarity in the wall layer increases afar from the wall, mainly owing to the shift toward higher frequencies of temperature fluctuations, in comparison with axial velocity fluctuations. Thus in this works the main goal is to look at the same phenomena, and with the same technique, at a turbulent plane Couette flow.

Thus the main goal of the present work has been to perform numerical experiments in a developed turbulent plane Couette flow and look at natural dissimilarity, and transport mechanisms in this kind of turbulence. It has been chosen a low Reynolds number equal to 1,300, as function of half the walls distance, h, and half the velocity of the moving wall, V_0, $Re_h = V_0 \rho h/\mu$, which gives a Reynolds number approximately of about 84 as a function of the friction velocity. The energy equation, on the other hand, is solved with isothermal boundary conditions. As in previous work for the fully developed turbulent channel flow, buoyancy effects were neglected, thus the temperature was considered as a passive scalar.

2 NUMERICAL METHOD

In this section a short description of the numerical aspects, and simulation parameters is given. A validation of the numerical code for a fully developed turbulent flow with heat transfer has been presented in a previous work (Pasinato, and Squires, 2006).

In this paper, u, v, and w are the instantaneous velocities in the streamwise (x), wall-normal (y), and spanwise (z) directions, respectively. All instantaneous variables are decomposed in a mean value and a fluctuation; e.g. $u = U + u'$. A plus symbol is used in order to denote nondimensionalization with the wall parameters, u_τ and ν; e.g. $y^+ = y\, u_\tau/\nu$.

The DNS of the turbulent plane Couette flow with heat transfer has been performed with periodic boundary condition in x and z directions. The size of the computational box, figure 2, which has a moving upper wall with velocity equal to $2V_0$, is $20\pi h \times 2h \times 4\pi h$ in x, y, and z directions, respectively. This box means 5270, and 1050 in wall units in x, and z directions, respectively. This computational domain is discretized with a $256 \times 72 \times 256$ grid, which in wall units means $\Delta x^+ = 20.6$, $\Delta y^+ = 0.57 - 4.04$, and $\Delta z^+ = 4.12$, in the three directions respectively. This computational box and discretization was chosen based on previous works in the literature, and some performed numerical tests, as it is commented in the next section.

The governing equations in dimensionless form are the continuity, the unsteady Navier-Stokes and energy equations for incompressible flow and heat transfer,

$$\frac{\partial u_i}{\partial x_i} = 0 \tag{1}$$

$$\frac{\partial u_i}{\partial t} + \frac{\partial}{\partial x_j}(u_j u_i) \;=\; \frac{1}{R_\tau}\frac{\partial^2 u_i}{\partial x_j \partial x_j} \;-\; \frac{\partial p}{\partial x_i} \tag{2}$$

$$\frac{\partial \theta}{\partial t} + \frac{\partial}{\partial x_j}(u_j \theta) \;=\; \frac{1}{Pr R_\tau} \frac{\partial^2 \theta}{\partial x_j \partial x_j} \tag{3}$$

where i and j are for $1, 2, 3$, and the non-dimensionalization used in the posprocessing of the results was done using the wall friction velocity, u_τ, half the distance between walls h, and the friction temperature $T_\tau = q_w/\rho\, c_p\, u_\tau$. Where θ is the dimensionless temperature, q_w is the heat flux at the wall, and c_p and ρ are the constant pressure specific heat coefficient and the density, respectively. In these equations Pr, and R_τ are the molecular Prandtl, the turbulent Reynolds numbers based on the wall friction velocity and half channel distance between walls, h, which values are 1 and approximately 84, repectively, as it is previously commented.

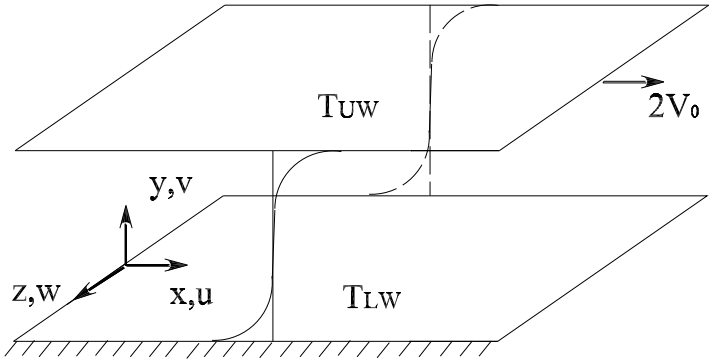

Figure 1: Computational domain for fully developed turbulent plane Couette flow with heat transfer.

The unsteady Navier-Stokes equations were solved numerically at a Reynolds number $Re_h = hV_0/\nu$ equal to 1300, which results in a R_τ of about 84, where V_0 is half the velocity of the moving wall. The numerical code used in the present work for the velocity fields was originally developed by Prof. Kyle Squires' group at ASU. In this code the incompressible momentum equation are discretized by the second-order accurate central-difference scheme. The Poisson equation for the pressure field is Fourier-transformed with respect to the streamwise and spanwise periodic directions and the resulting three-diagonal equations are solved directly for each time step. The flow field is advanced in time using a fractional-step method (Kim and Moin, 1985), with the Crank-Nicolson second-order scheme for the viscous terms and the Adams-Bashforth scheme for the non-linear terms. Periodic boundary conditions are used for the homogeneous x (streamwise), and z (spanwise) directions, respectively. And non-slip boundary conditions at both walls.

After the velocity field is calculated at each time step, the temperature field is obtained integrating the energy equation. Any buoyancy effect was neglected, thus temperature was considered as a passive scalar. The thermal field is solved with the same space, and time discretization, and same numerical scheme used for the velocity field. As boundary conditions, constant wall temperature was used with a hot upper wall, and a cold lower wall.

The time step was $0.01h/V_0$ or $0.05\nu/u_\tau^2$, and the time integration was taken approximately equal to $400h/V_0 = 2,200\nu/u_\tau^2$, in order to define mean values.

3 RESULTS AND DISCUSSION

3.1 Mean values

Study	Re_τ	$N_x \times N_y \times N_z$	L_x/h	L_z/h	Δx^+	Δz^+	Δy^+
Lee and Kim (1991)	170	$192 \times 129 \times 288$	4π	$8/3\pi$	11.1	4.9	
Kristoffersen at al. (1993)	83.2	$96 \times 64 \times 64$	4π	2π	10.9	8.2	0.2-0.4
Papavassiliou and Hanratty (1994)	150	$128 \times 65 \times 128$	4π	2π	14.8	7.4	
Bech et al. (1995)	82.2	$256 \times 70 \times 256$	10π	4π	10.1	4.0	0.7 - 3.9
Komminaho at al (1996)	52.2	$256 \times 70 \times 256$	28π	8π	13.5	7.7	1.9 - 1.9
Debusschere and Rutland(2004)	186	$231 \times 200 \times 64$	12	2	8.3	5.1	1.6 - 1.6
Present	83.2	$256 \times 73 \times 256$	20π	4π	20.4	4.08	0.5 - 4.1

Table 1: Comparison of domain size and discretization with previous studies.

As it was commented in the introduction, plane Couette flow has proved to be more difficult to simulate, due to the existence of very large streamwise structures in the center region of the flow in numerical simulations. Several simulations have revealed these long streamwise vortical structures at the centerline of the plane turbulent Couette flow. However there are doubts yet that these structures can be physical or only a spurious numerical problem. For example Andersson, Lygren, and Kristoffersen (1998) have not observed experimentally these structures, and suggested that such kind of secondary flow can be a numerical spurious flow phenomenon, owing to the self-amplification that can produce periodic boundary conditions.

As a consequence of this situation, in this work, special care was taken in order to define the box size. In table 1 a list of different DNSs of turbulent plane Couette flow is given, together with details of the computational parameters. Also in this Table is the box size and discretization finally used in the present work, which has almost the same Re_h and discretization of the numerical simulation performed by Bech et al. (1995). The only difference between both simulations is the axial size of the computational domain, and therefore the axial discretization. However in the present work an axial length of 20π, based on the streamwise two-point correlation coefficients, was defined as the minimum axial size of the computational domain in order to have a decorrelation of axial structures, as it is explained below.

Figures 2(a)-2(b)-2(c), and 2(d) present the streamwise and spanwise two-point correlation coefficients, at two positions from the wall $-$ one close to the wall at $y^+ = 5$, and the second in the center region at $y^+ = 72\ -$. In these figures, the two-point correlations in $x-$ and $z-$ directions at two $y-$locations show that they fall off to zero values for large separations, indicating that the computational domain is suffriciently large. From figures 2(a)-2(b) it is clear the streamwise decorrelation of axial velocity at the middle of the computational domain, where there are the expected elongated streamwise structures.

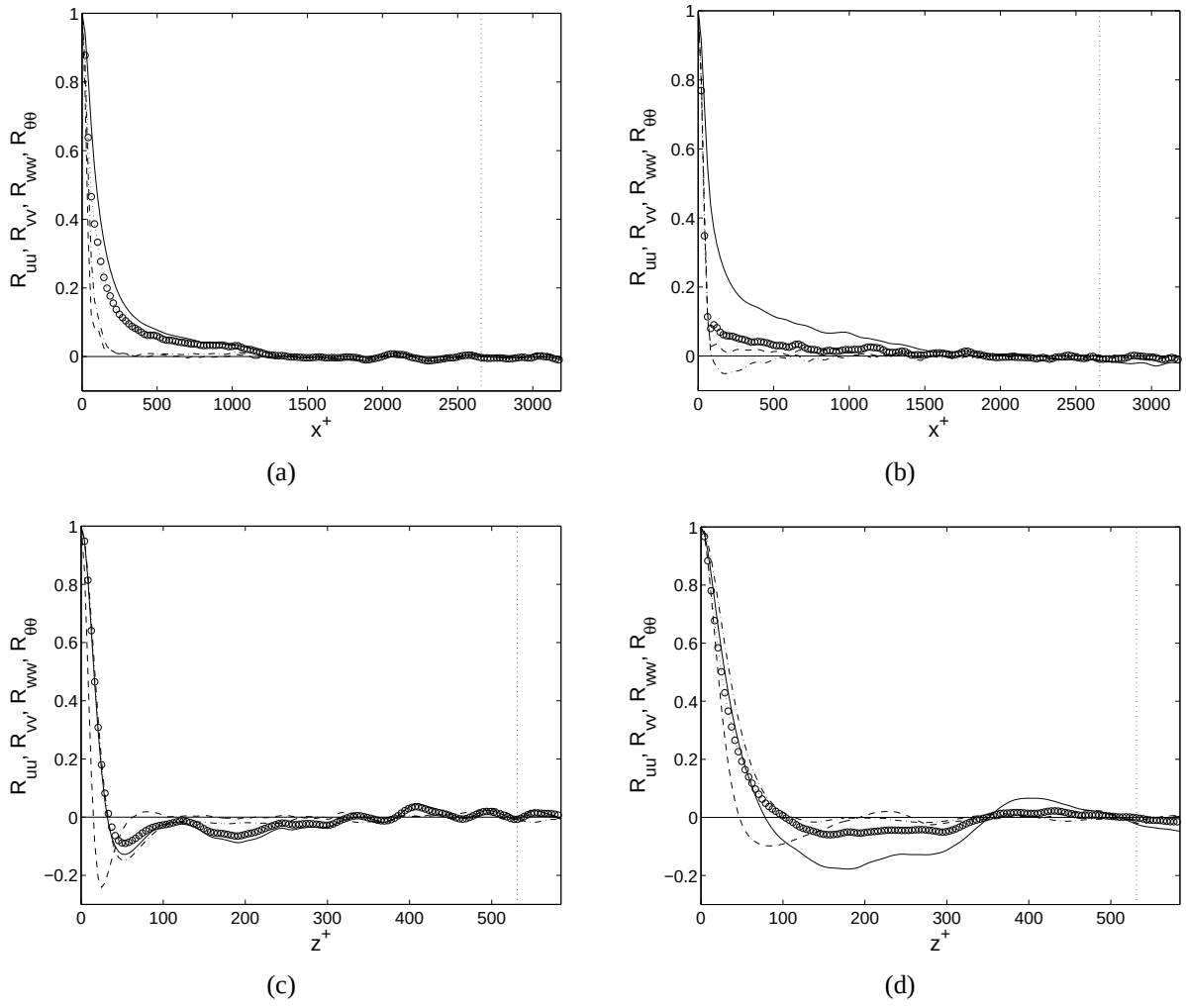

Figure 2: Two-point streamwise, and spanwise, correlation coefficients, $R_{uu};\ R_{vv};\ R_{ww};\ R_{\theta\theta}$, in the near-wall region at $y^+ = 5$, (a-c), and in the center region at $y^+ = 72$, (b-d). Solid line, R_{uu}; $\circ\cdots\circ\cdots\circ$, $R_{\theta\theta}$; $---$, R_{vv}; $-.-.-$, R_{ww}. Dotted line denotes half the computational domain.

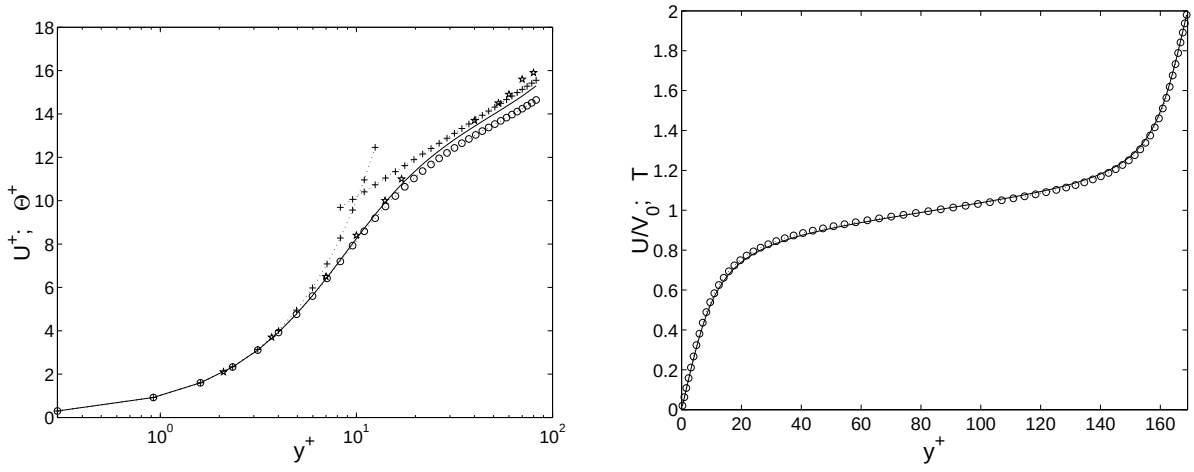

(a) (b)

Figure 3: Distribution of mean velocity and temperature for fully developed turbulent plane Couette flow with $Re_h = 1,300$ and $Pr = 1$. (a) Solid line, mean velocity; $\circ \cdot\cdot \circ \cdot\cdot \circ$, mean temperature; $+ \cdot\cdot + \cdot\cdot +$, $U^+ = y^+$ and $2.55\ ln(y^+) + 4.3$; $\star \cdot\cdot \star \cdot\cdot \star$, Exp. values, Bech et al. (1995). (b) Solid line, mean velocity; $\circ \cdot\cdot \circ \cdot\cdot \circ$, mean temperature.

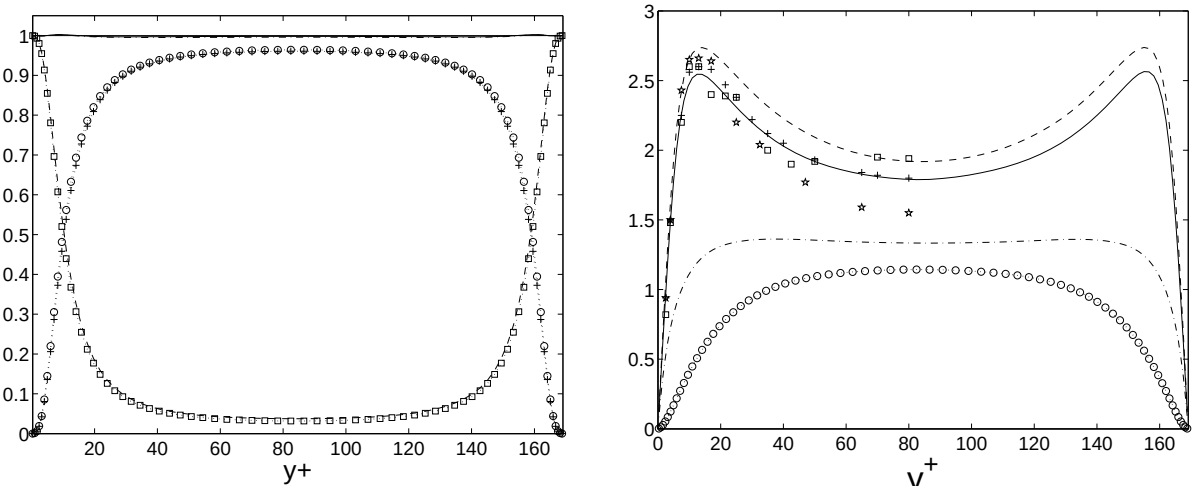

(a) (b)

Figure 4: Distribution of Reynolds, thermal stresses, and rms for turbulent Couette flow with $Re_h = 1,300$ and $Pr = 1$. (a) Solid line, Total stresses; $+ \cdot\cdot + \cdot\cdot +$, $-\langle u'v' \rangle$; $-.-.-$, dU^+/dy^+; $\cdot - \cdot - \cdot - \cdot$, Total thermal stress; $\circ \cdot\cdot \circ \cdot\cdot \circ$, $-\langle v'\theta' \rangle$; $\square \cdot\cdot \square \cdot\cdot \square$, $d\theta^+/dy^+$. (b)Solid line, u'_{rms}; $\circ \cdot\cdot \circ \cdot\cdot \circ$, v'_{rms}; $\cdot - \cdot - \cdot - \cdot$, w'_{rms}; $- - -$, θ'_{rms}; $+ \cdot\cdot + \cdot\cdot +$, DNS, Bech et al(1995); $\star \cdot\cdot \star \cdot\cdot \star$, exp., Bech et al(1995); $\square \cdot\cdot \square \cdot\cdot \square$, Aydin and Leutheusser (1991).

Figures 3(a)-3(b), on the other hand, show the distribution of dimensionless mean velocity and temperature. The mean velocity in the center of the channel is underpredicted by a 3% in comparison with the experimental data of Bech et al. (1995). And figures 4(a)-4(b) show the Reynolds, thermal stresses, and root mean square, rms, of velocity and temperature fluctuations. Figure 4(b) shows the comparison of the rms of the axial velocity, with DNS and experimental data with relatively good agreement. Figure 4(a) reveals that wall normal turbulent transport of axial momentum and heat are almost the same for the whole flow.

Therefore, previous results reveal that the developed plane turbulent Couette flow for $Re_h = 1,300$, with computational domain of $20\pi h \times 2h \times 4\pi h$ and discretization of $256 \times 73 \times 256$, is well resolved in the mean and turbulent values.

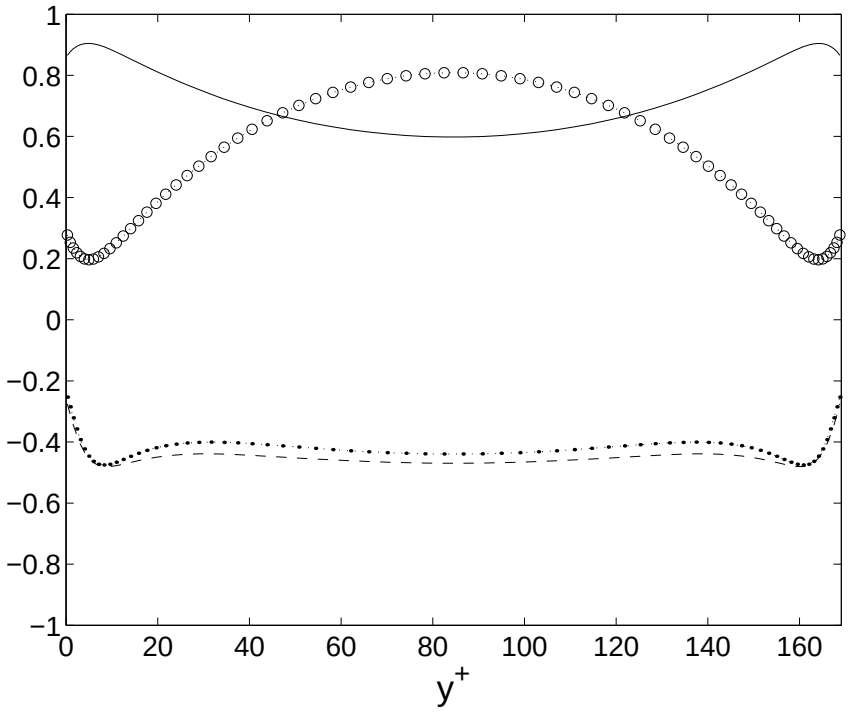

Figure 5: Wall normal distribution of correlation coefficients, for developed plane Couette turbulent flow with $Re_h = 1,300$. Solid line, $\rho_{(u'\theta')}$; $\circ \cdots \circ \cdots \circ$, $d_{(u'\theta')}$; $- - -$, $\rho_{(v'\theta')}$;; $\cdots\cdots$, $\rho_{(u'v')}$;.

3.2 Dissimilarity from most energetic events

One of the reason the plane turbulent Couette flow is a unique test case in order to study axial velocity and temperature similarity, is the analogy between Reynolds-averaged axial momentum and energy equations. These equations are,

$$0 = \frac{1}{R_\tau}\frac{d^2U}{dy^2} - \frac{d}{dy}\langle u'v'\rangle \tag{4}$$

$$0 = \frac{1}{PrR_\tau}\frac{d^2\Theta}{dy^2} - \frac{d}{dy}\langle \theta'v'\rangle \tag{5}$$

where the mean values are defined along the $x - z$ plane and time.

As it is seen from dimensionless equations (4 - 5), for the special case of $Pr = 1$, these equations, as its boundary conditions for heat transfer in Couette flow with wall constant temperature, are analogous. Thus subtracting equation (5) from equation (4), it results in,

$$0 = \frac{1}{PrR_\tau}\frac{\partial^2\Phi}{\partial y \partial y} - \frac{\partial}{\partial y}\langle\phi' v'\rangle \tag{6}$$

where $\Phi = U - \Theta$, and $\phi' = u' - \theta'$.

Therefore, as it was proposed in a previous work (Pasinato, 2007) in which the natural dissimilarity in a fully developed turbulent channel flow was studied for $Pr = 1$, for convenience the difference of instantaneous dimensionless axial velocity and instantaneous dimensionless temperature $\phi = u - \theta$ is used as a measure of dissimilarity in the analysis of results. In other words, the new variable is, as all instantaneous variables, the sum of a mean and a fluctuating value, $\phi = \Phi + \phi' = (U - \theta) + (u' - \theta')$. And the variance of ϕ, normalized by the product of the rms of axial velocity and temperature, u^+, θ^+, is used as a normalized measure of dissimilarity of fluctuating values, as the correlation coefficient is a normalized measure of the correlation of fluctuating values,

$$d_{(u'\theta')} = \frac{\langle\phi'^2\rangle}{u^+\theta^+} = \frac{\langle u'u'\rangle - \langle u'\theta'\rangle}{u^+\theta^+} + \frac{\langle\theta'\theta'\rangle - \langle u'\theta'\rangle}{u^+\theta^+} \tag{7}$$

where $d_{(u'\theta')}$ is zero when correlation coefficient $\rho_{(u'\theta')} = 1$.

Figure 5 shows the distribution of $d_{(u'\theta')}$ according to equation (7), and also shows the distribution of the correlation coefficients $\rho_{(u',\theta')}$, $\rho_{(u',v')}$, and $\rho_{(\theta',v')}$. It is clear from this figure that dissimilarity is minimum at the top of the viscous layer, approximatley $y^+ = 5$, as the correlation coefficient is maximum at this point. On the other hand, dissimilarity is maximum at the center region of the flow, in contrast with the correlation coefficient that is minimum there. But, why it used this new measure of axial velocity and temperature fluctuations difference? Why it is not used the instantaneous second moment $u'\theta'$ as a measure of similarity? And the answer is that it seems more conveniente, for analysis reason, to look at a function which is the difference of other two functions, rather than at one that is the product of them.

According to the mean values definition in the present work for a developed turbulent Couette flow, the Reynolds averaged form of the mean dissimilarity is the results of the balance between diffusion and the wall normal gradient of Reynolds and thermal stress,

$$0 = \frac{1}{R_\tau}\frac{d^2\Phi}{dy^2} - \frac{d}{dy}(\langle u'v'\rangle - \langle v'\theta'\rangle) \tag{8}$$

Reynolds and thermal stress, however, have almost the same distribution across the flow according to figure 4(a), thus Φ should have an almost linear ditribution in $y-$direction for developed turbulent Couette flow.

Then in the following of this section the contribution to dissimilarity between axial velocity and temperature fluctuations, due to natural phenomena occurring in the wall layer, is studied with the same approach used in Pasinato (2007), which uses the new variable ϕ in the analysis. For completeness reasons the basic of the approach is repeated here. Note that all values of velocity and temperature fluctuations, and moments, are dimensionless values, and that $Pr = 1$ for the data used in the numerical experiment here.

Thus the idea in this subsection is to detect an event characterized as *important dissimilarity event* with some algorithm and evaluate their mean contribution to the mean dissimilarity, as it

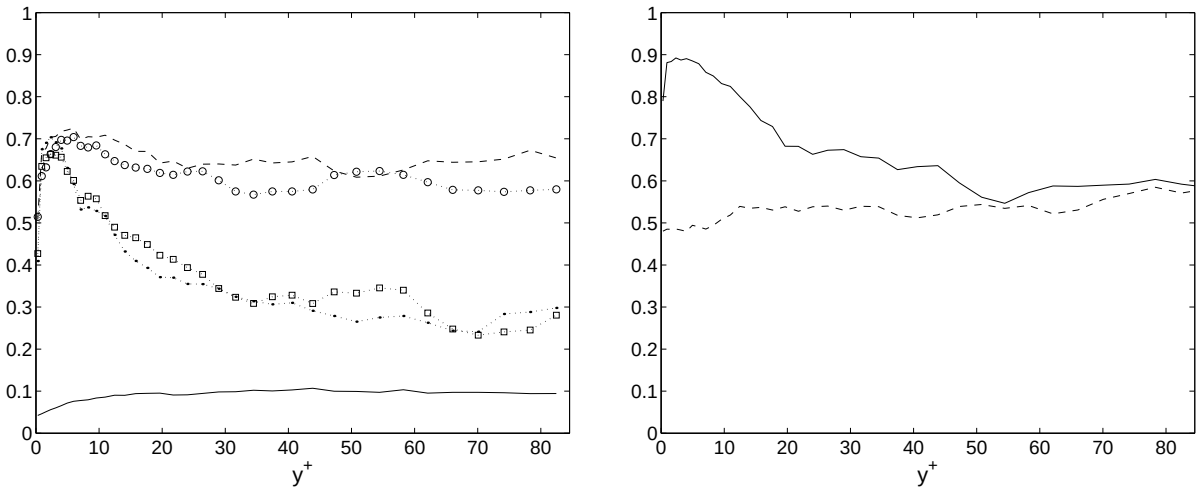

(a) (b)

Figure 6: Probability of the most energetic events in the wall layer for a plane turbulent Couette flow with heat transfer, with $Re_h = 1300$, and $Pr = 1.0$, that satisfy the following conditions. (a) Solid line, $P(\widehat{\phi'^2} - \bar{\phi}^2 \geq k\phi^{+2})$; $- - -$, $P(\widehat{\phi'^2} - \bar{\phi}^2 > k\phi^{+2},\ \widehat{u'v'} < 0)$; $\circ \cdot \cdot \circ \cdot \cdot \circ$, $P(\widehat{\phi'^2} - \bar{\phi}^2 > k\phi^{+2},\ \widehat{\theta'v'} < 0)$; $\cdot \cdot \cdot \cdot \cdot$, $P(\widehat{\phi'^2} - \bar{\phi}^2 > k\phi^{+2},\ \widehat{u'v'} < 0, \widehat{v'} < 0)$; $\square \cdot \cdot \square \cdot \cdot \square$,$P(\widehat{\phi'^2} - \bar{\phi}^2 > k\phi^{+2},\ \widehat{\theta'v'} < 0, \widehat{v'} < 0)$.(b) Solid line, $P(\widehat{\phi'^2} - \bar{\phi}^2 > k\phi^{+2},\ \widehat{u'v'} < 0,\ \widehat{\theta'v'} < 0)$; $- - -$, $P(\widehat{\phi'^2} - \bar{\phi}^2 > k\phi^{+2},\ \widehat{\partial p'/\partial x} < 0)$.

was defined in equation (7). As detection algorithms for an *important dissimilarity event*, one analogous to those used in the literature to detect burst or ejection events, was used. The most common of these algorithms are the uv quadrant 2, the variable interval time average (VITA), and the $u-$label techniques. And they have been used in order to investigate burst period and high pressure peaks frequency in wall turbulence (Lu and Willmarth, 1973; Blackwelder and Haritonidis, 1983; Luchik and Tiederman, 1987; Shah and Antonia 1988; Johansson, Her, and Haritonidis 1987).

Although there is not doubts that the most important dissimilarity events in the wall layer are produced by events like as burst or ejection, and sweeping motions, in this work, however, the idea is not to detect these events and then evaluate the dissimilarity associated to them. On the contrary, the idea is to detect the most important instantaneous oscillations in ϕ, and then evaluate their importance in the production of mean dissimilarity. Of course that at the same time that an important event is detected, it is detected also which kind of events - sweeping motin, ejection, etc - are associated with it. In other words, in this works two or three important dissimilarity events are detected and its dissimilarity contribution is evaluated, not matter they belong or not to the same burst, ejection or sweeping motion events.

Then the algorithms used to detect events that yields an important dissimilarity, based on the VITA and the second quadrant algorithms, detect one event when the variance of the fluctuation of ϕ is,

$$\widehat{\phi'^2} - \bar{\phi}^2 \ \geq \ k\phi^{+2} \tag{9}$$

where the mean values $\bar{\phi}$, and rms ϕ^+ are evaluated from the whole sample, and the wide-hat symbol means a mean values in the time filtering interval T,

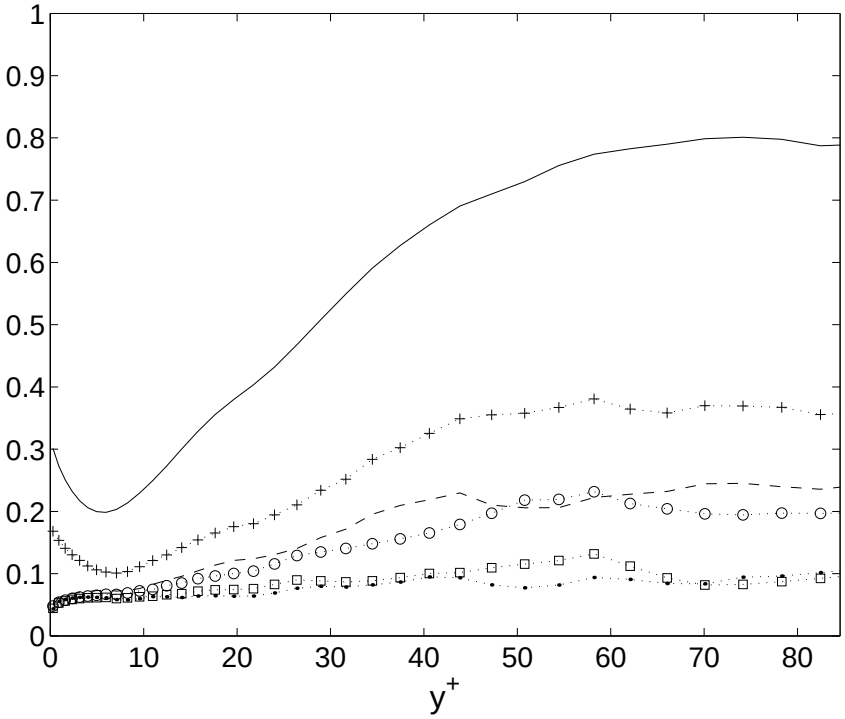

Figure 7: Dissimilarity contribution of the most energetic events in the wall layer for a plane turbulent Couette flow with heat transfer, with $Re_h = 1300$, and $Pr = 1.0$, that satisfy the following conditions. (a) Solid line, Total dissimilarity of the whole sample; $+\cdots+\cdots+$, $P(\widehat{\phi'^2} - \bar{\phi}^2 \geq k\phi^{+2})$; $---$, $P(\widehat{\phi'^2} - \bar{\phi}^2 > k\phi^{+2},\ \widehat{u'v'} < 0)$; $\circ\cdots\circ\cdots\circ$, $P(\widehat{\phi'^2} - \bar{\phi}^2 > k\phi^{+2},\ \widehat{\theta'v'} < 0)$; $\cdots\cdots$, $P(\widehat{\phi'^2} - \bar{\phi}^2 > k\phi^{+2},\ \widehat{u'v'} < 0, \widehat{v'} < 0)$; $\square\cdot\square\cdot\square$,$P(\widehat{\phi'^2} - \bar{\phi}^2 > k\phi^{+2},\ \widehat{\theta'v'} < 0, \widehat{v'} < 0)$.

$$\widehat{\phi(t,T)'} \ = \ \frac{1}{T}\int_{t-T/2}^{t+T/2} \phi'(\tau)d\tau \tag{10}$$

The algorithms above have two parameters, the filtering time period T and the threshold k. k was taken equal to 2.5 based on the pdf of ϕ (values of ϕ out of the interval $\pm 2.5\phi^{+}$), using the same criteria used in Pasinato (2007) for a turbulent channel flow. As regarding the second parameter, the filtering period T, this period in dimensionless form used in this work was $T^{+} \approx 1.2$, which is out the range, $6 \ < \ T^{+} = tu_{\tau}^{2}/\nu \ < \ 13$, for dimensionless burst period found in the literature. On the other hand, because the mean and the rms values of ϕ, ϕ^{+} and $\bar{\phi}$, used in the algorithms are evaluated for the whole sample, the algorithms can be used for instantaneous values without any filter. Moreover, numerical tests were done which shown that results were only slightly sensible to the filtering period for values of $T^{+} < 10$.

Therefore, using the algorithms above, once an event that qualify as important dissimilarity event was detected, conditional probability with different conditions were used in order to characterize whether these events with strong dissimilarity in axial velocity and temperature, satisfy a second, or a second and a third condition. Some of the conditions used were,

$$P(\widehat{\phi'^2} - \bar{\phi}^2 > k\phi^{+2}, \widehat{u'v'} < 0) \tag{11}$$

aiming at to detect how many of the events detected as important dissimilarity events, also belong to events in the second quadrant, Q2.

$$P(\widehat{\phi'^{\,2}} - \bar{\phi}^2 > k\phi^{+2}, \widehat{u'v'} < 0, \widehat{v'} < 0) \tag{12}$$

aiming at to detect events characterized as important dissimilarity events, that belong to Q2, for which the wall normal velocity is negative (sweeping motion).

$$P(\widehat{\phi'^{\,2}} - \bar{\phi}^2 > k\phi^{+2}, \widehat{\partial p'/\partial x} < 0) \tag{13}$$

$$P(\widehat{\phi'^{\,2}} - \bar{\phi}^2 > k\phi^{+2}, \widehat{\partial p'/\partial x} > 0) \tag{14}$$

aiming at to detect whether dissimilarity is associated with local instantaneous favorable or adverse axial pressure gradient.

Then figures 6(a)-6(b)-7 show the results of this section. Figure 6(a) shows that the probability of the events characterized as important dissimilarity events, is approximately constant along the whole flow between plates and close to 10%. This means that the number of events with strong dissimilarity in the wall layer for a developed turbulent Couette flow are only a 10% of the total. This figure shows also that 70% of events that produce dissimilarity belong to Q2 quadrant for velocity, and almost the same percentage belong to the Q2 quadrant for temperature. And moreover these values for both velocity and temperature are aproximately constant along the whole flow. However, from these events that belong to Q2 quadrant in both fields, the probability of those that are sweeping motions, or inrushes of hot fluid with high momentum toward the walls, decreases toward the centerline of the flow, from 70% at the wall to a 30% percent at the centerline. In other words, it is seen that the inrushes or movements of high momentum toward the wall are felt in the whole flow, and that the number of events detected with this condition is more or less equal to 70% in the viscous layer, decreasing slowly afar from the wall. On the other hand, figure 6(b) shows that not all events that yields important dissimilarity are in Q2 quadrant for velocity, and at the same time in Q2 quadrant temperature. At the centerline only a 60% of events in Q2 quadrant for velocity are also in Q2 quadrant for temperature. As regards the instantaneous local pressure gradient, figure 6(b) shows that it is not a direct link at all to velocity and temperature fluctuations dissimilarity.

Figure 7 in first place shows that the sample used in the analysis of event detection, have the same distribution of mean dissimilarity $d_{(u'\theta')}$ to that from the whole period of time integration for definition of mean values (figure 5). And shows also that the contribution to dissimilarity $d_{(u'\theta')}$ from the most energetic events is nearly constant from the wall to the centerline, close to or something less than 50%. Other interisting result from figure 7 is that the major part of the contribution to $d_{(u'\theta')}$ by the most energetic events are from events of the Q2 quadrant. And from this last contribution, the sweeping motions toward the wall account for a 50% in the center region of the flow, and for the total at the wall. In other words, at the very near-wall sweeping motions are responsable for almost all dissimilarity associated with most energetic events.

These are basically the most important results from the analysis in this section. And it can be concluded that for developed turbulent Couette flow, as it is for developed turbulent channel flow, it is the background turbulence the main source of natural dissimilarity between velocity and temperature fluctuations. In the next section a short analysis in the frequency domain is done in order to see how the energy of the fluctuations of ϕ, or oscillations of velocity and temperature differences, change from the wall to the centerline of the flow.

3.3 Dissimilarity analysis in the frequency domain

Figures 8, 9(a), and 9(b) show the spectra for the fluctuations of velocity components, temperature, the difference between axial velocity and temperature, ϕ, and pressure, normalized by their rms, at four positions from the wall. These position are at $y^+ = 5$, or final of the viscous layer, $y^+ = 16$, or buffer region, $y^+ = 30$, or beginning of the logarithmic region, and $y^+ = 72$, or center region of the flow. There were selected these four positions because they give a more or less complete picture of the spectra modification in the wall layer. In these figures is plotted the decimal logarithmic of $\omega\delta/u_\tau$ in the abscissa, and the product of $(\omega\delta/u_\tau)\Phi_a$ in ordinate, where Φ_a is the spectral density function of the variable a normalized to unity. The area under any section of figures 8, 9(a), and 9(b) is proportional to the fraction of total $\langle a'^2\rangle/a^{+2}$ in that particular frequency range. In other words, the spectra show the energy distribution of the normalized fluctuations.

Figure 8 shows the spectra of u', and θ', and its difference, at the four positions. From this figure it is clear a shift toward higher frequencies of all spectra, but mainly of ϕ', and thus θ'. And this difference increases quickly in the first three positions from the wall. Then this tendency decreases slightly toward the center region. In both spectra for velocity and temperature, as position y^+ increases for the first three positions, the peaks decreases as its position change toward higher frequencies. This results agree with was found by Antonia et al. (1987), who did observations in a heated turbulent boundary layer for $y^+ < 40$. Then at the center of the flow in figure 8 the peaks of u' and θ' spectra increases in comparison to those in the beginning of logarithmic layer, $y^+ = 30$.

On the other hand, figure 9(a) shows the spectra for v', w', and ϕ'. And figure 9(b) shows a comparison of previous spectra of u' and θ' with p' spectrum. From these figures it is clear the energy distribution generated by instantaneous pressure gradient. And it seems that the wall normal velocity component produces the major part of axial velocity and temperature fluctuations dissimilarities, taking energy from the streamwise velocity through the instantaneous pressure gradient.

Therefore, a picture of axial velocity and temperature fluctuations in the frequency domain is that the whole kind of turbulent events in the wall layer yields a gradual de-correlation, taken energy form velocity and injecting it in temperature mainly trough wall normal velocity, and in second place by spanwise velocity. Although it seems that spectra have a convergence toward the center of the flow, axial velocity has always its maximum energy at lower frequencies. Although it seems to be a simple picture explained in most turbulence text book (Tennekes, and Lumly, 1972), the previous analysis gives information that will be worth in future numerical experiments, and heat transfer modeling in turbulent flows.

4 CONCLUSION

A direct numerical simulation, DNS, of a fully developed turbulent plane Couette flow with heat transfer has been performed. The main goal was to look at natural dissimilarity, and axial momentum and thermal energy transport mechanism in this kind of turbulence. The Reynolds number, Re_h, is 1,300 as a function of half the walls distance and half the velocity of the moving wall. This Re_h gives a Reynolds as a function of half walls distance and friction velocity, Re_τ, of about 84. The energy equation was solved for a molecular Prandtl number, Pr, equal 1, and with isothermal boundary conditions at both walls. The temperature was considered as a passive

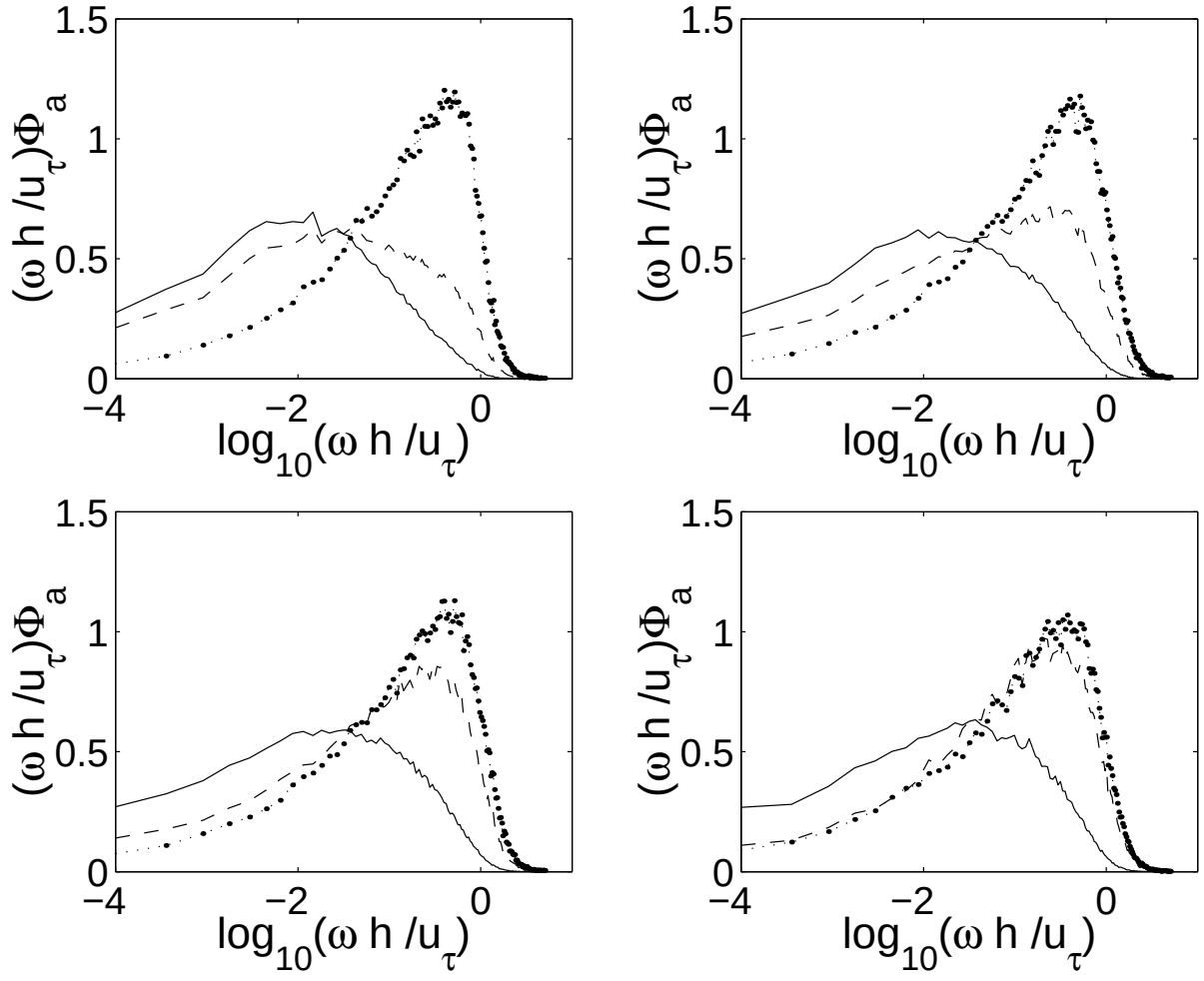

Figure 8: Frequency analysis of dissimilarity for a developed turbulent Couette flow with heat transfer, for $Re_h = 1300$, and $Pr = 1.0$. Spectral density function of u', θ', and ϕ', at four positions from the wall, (top-left) $y^+ = 5$; (top-right) $y^+ = 16$; (bottom-left) $y^+ = 32$; (bottom-right) $y^+ = 72$. Solid line, $a = u'/u^+$; $- - -$, $a = \theta'/\theta^+$; $\cdots\cdots$, $a = \phi'/\phi^+$.

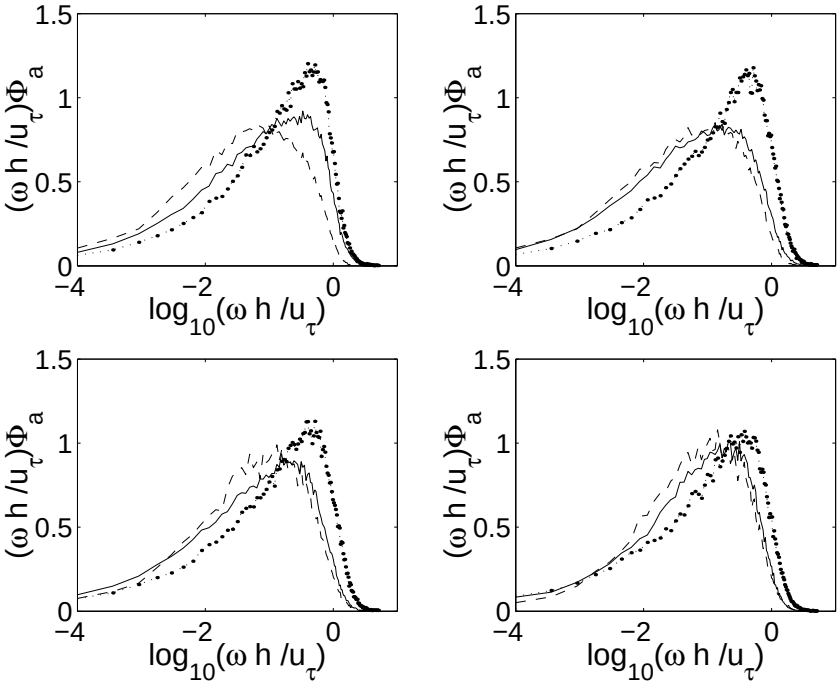

(a)

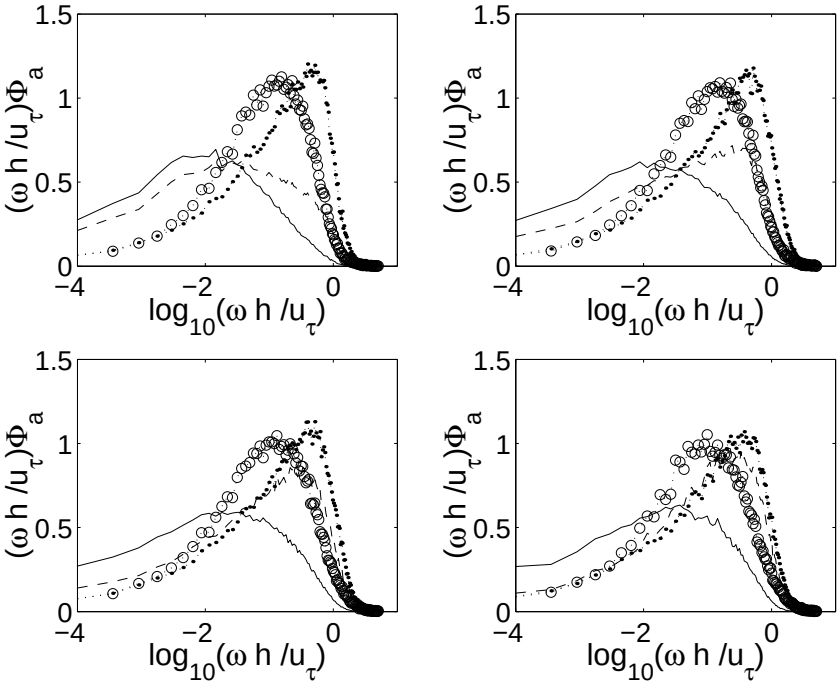

(b)

Figure 9: Frequency analysis of dissimilarity for a developed turbulent Couette flow with heat transfer, for $Re_h = 1300$, and $Pr = 1.0$. (a) Spectral density function of v', w', and ϕ', at four positions from the wall, (top-left) $y^+ = 5$; (top-right) $y^+ = 16$; (bottom-left) $y^+ = 32$; (bottom-right) $y^+ = 72$. Solid line, $a = v'/v^+$; $- - -$, $a = w'/w^+$; $\cdots\cdots$, $a = \phi'/\phi^+$. (b) Spectral density function of u', θ', ϕ' and p', at four positions from the wall, (top-left) $y^+ = 5$; (top-right) $y^+ = 16$; (bottom-left) $y^+ = 32$; (bottom-right) $y^+ = 72$. Solid line, $a = u'/u^+$;$- - -$, $a = \theta'/\theta^+$; $\cdots\cdots$, $a = \phi'/\phi^+$; $\circ\cdots\circ\cdots\circ$, $a = p'/p^+$.

scalar.

The main results of this work show that axial velocity and temperature fluctuations have the same kind of natural dissimilarity present in turbulent channel flow. While natural decorrelation between axial velocity and temperature starts in the very near-wall region due to the most energetic events there, the contribution of these events to the total natural dissimilarity is less than fifty percent in the whole flow.

Analysis of longitudinal velocity and temperature fluctuations in frequency domain, using spectral density functions, shows that the main cause of natural dissimilarity is the shift toward higher frequencies of temperature in comparison to axial velocity, in the viscous, buffer, and beginning of the logarithmic region. Based on the spectra of pressure and wall normal fluctuations, it is clear that wall normal velocity, which receives energy from axial velocity through the pressure field, plays an important role in the natural dissimilarity of streamwise velocity and temperature fluctuations.

Therefore, the contribution to dissimilarity of the most energetic events in the wall layer is important, but do not explain the major causes of correlation degradation between axial velocity and temperature fluctuations toward the center of the flow. Neither they explain the major fraction of dissimilarity in the viscous and buffer regions where these events are the strongest. This result is the same obtained for turbulent channel flow. As it was verified in a previous work for developed turbulent channel flow (Pasinato, 2007), for developed plane turbulent Couette flow, the wall normal velocity plays a fundamental role in the axial velocity and temperature fluctuations dissimilarity. In other words, it is through wall normal velocity that thermal field receives most energy from the longitudinal velocity. This is a simple picture that is explained in most book on fundamental aspects of turbulence, however the analysis presented here gives information possible to be used in future numerical experiments, or heat transfer modeling in perturbed turbulent flows.

ACKNOWLEDGMENT

This work was partially sponsored by the Air Force Office of Scientific Research under Grant No. FA9550-07-1-0393.

REFERENCES

Andersson H.I., M. Ligren, and R. Kristoffersen. Roll cells in turbulent plane Couette flow: Reality or artifact? *Proc. of the Sixteenth Int. Conf. on Numerical Methods in Fluid Dynamics*. Springer-Verlag, Berlin, pp. 117-122, 1998.

Aydin E.M., and H.J. Leutheusser. Plane-Couette flow between smoth and rough walls. *Exp. Fluids*, **11**, pp. 302-312, 1991.

Akselvoll K., and P. Moin. Large-Eddy simulation of turbulent confined coannular jets and turbulent flow over a backward facing step. Report TF-63, Thermoscience Division, Department of Mechanical Engineering, Stanford University, 1995.

Antonia R.A., H.Q. Danh and a. Prabhu. Response of a turbulent boundary layer to a step change in surface heat flux. *J. Fluid Mech.*, **80**, 153, 1977.

Antonia R.A. and H.Q. Danh. Structure of temperature fluctuations in a turbulent boundary layer. *Physics of Fluids*, **20**(7), 1050-1057, 1977.

Antonia R.A. Behavior of the turbulent Prandtl number near the wall. *Int. J. Heat Mass Transfer*, **23**, 906-908, 1980.

Antonia R.A., L.V. Krishnamoorthy, and L. Fulachier. Correlation between the longitudinal velocity fluctuation and temperature fluctuation in the near-wall region of a turbulent boundary layer. *Int. J. Heat Mass Transfer*, **31**(4), 723-730, 1987.

Bech K.H., N. Tillmark, P.H. Alfredsson, and H.L. Andersson. An investigation of turbulent plane Couette flow at low Reynolds numbers, *J. Fluid Mech.*. **286**, 291-325, 1995.

Blackwelder R.F., and J.H. Haritonidis. Scaling of the bursting frequency in turbulent boundary layers. *J. Fluid Mech.*. **132**, pp. 87, 1983.

Debusschere B., and C.J. Rutland. Turbulent Scalar Transport Mechanisms in Plane Channel and COuette Flows. *J. Fluid Mech.*, 2000.

Fulachier L. and R. Dumas. Spectral analogy between temperature and velocity fluctuations in a turbulent boundary layer. *J. Fluid Mechanics*, **77**, 257-277, 1976.

Hamilton J.M., J. Kim, and F. Waleffe Regeneration mechanism of near-wall turbulence structures. *J. Fluid Mech.*, **287**, 317-348, 1995.

Hishida M., and Y. Nagano. Structure of turbulent velocity and temperature fluctuations in fully developed pipe flow, *J. Heat Transfer*. **101**, 15-22, 1979.

Inaoka J., J. Yamamoto, and K. Suzuki. Dissimilarity between heat transfer and momentum transfer in a disturbed turbulent boundary layer with insertion of a rod - modeling and numerical simulation. *Int. J. Heat Fluid Flow*, **20**, 290-301, 1999.

Iritani Y., N. Kasagi, and M. Hirata. Heat transfer mechanism and associated turbulence structure in the near wall region of a turbulent boundary layer, in *Turbulent Shear Flow*. **4**, 223-234, 1985.

Johansson A.V., J.Y. Her, and J.H. Haritonidis. On the generation of high-amplitude wall-pressure peaks in turbulent boundary layer and spots. *J. FLuid Mech*, **176**, pp. 119-142, 1987.

Kasagi K., Y. Tomita, and A. Kuroda. Direct numerical simulation of the passive scalar field in a turbulent channel flow. *Transaction of ASME, Journal of Heat Transfer*, **114**, 598-606, 1992.

Kasagi N. and Y. Ohtsubo. Direct numerical simulation of low Prandtl number thermal field in a turbulent channel flow. In *Turbulent Shear Flow*, **8**, 97-119, 1993.

Kawamura H., H. Abe, and Y. Matsuo. DNS of turbulent heat transfer in channel flow with respect to Reynolds and Prandtl number effects. *Int. J. Heat Fluid Flow*, **20**, 196-207, 1999.

Kim J., and P. Moin. Application of a fractional-step method to incompressible Navier-Stokes equations. *J. Comp. Physics*, **59**, pp. 308-323, 1985.

Kim J., and P. Moin. Transport of Passive Scalar in a Turbulent Channel Flow. In *Turbulent Shear Flow*, **6**, 86-96. 1989.

Komminaho J., A. Lundbladh, and A. Johansson. Very large structure in plane turbulent Couette flow. *J. Fluid Mech.*, **320**, 259-285, 1996.

Kong H., H. Choi, and J.S. Lee.Dissimilarity between the velocity and temperature fields in a perturbed turbulent thermal boundary layer. *Physics of Fluids*, **13**(5), 1466-1479, 2001.

Luchik T.S. and W.G. TIederman. Timescale and structure of ejections and bursts in turbulent channel flows *Journal of Fluid Mechanics*. **174**, 529-552, 1987.

Lu S., and W.W¿ Willmarth. Measurements of the structure of Reynodsl stress in a turbulent boundary layer. *Journal of Fluid Mechanics*. **60**, pp. 481, 1973.

Na Y., D.V. Papavasiliou, and T. J. Hanratty. Use of direct numerical simulation to study the effect of Prandtl number on temperature fields. *Int. J. Heat and Fluid Flow*, **20**, 187-195, 1999.

Nagano Y. and M. Tagawa. Statistical characteristics of wall turbulence with a passive scalar, *Journal of Fluid Mechanics*. **196**, 157-185, 1988.

Pasinato H.D., and K. Squires. On the Effect of Perturbed Channel Flow on Thermal Field, *ENIEF2006*, Santa Fe, 2006.

Pasinato H.D. Velocity and Temperature Natural Dissimilarity in a Turbulent Channel Flow, *Mecánica Computacional*, **XXVI**, pp. 3644-3663; S.A. Elaskar, E.A. Pilotta, and G.A. Torres (Eds); Córdoba, Argentina, 2007.

Shah D.A. and R.A. Antonia. Scaling of the ”bursting” period in turbulent boundary layer and duct flows. *Physics of Fluids A*, **1**(2), 318-325, 1989.

Spalart P.R. and M.K. Strelets. Mechanisms of transition and heat transfer in a separation bubble, *Journal of Fluid Mechanics*. **403**, 329-349, 2000.

Subramanian C.S. and R.A. Antonia. Effect of Reynolds number on a slightly heated turbulent boundary layer. *Int. J. Heat Mass Transfer*, **24**(11), 1833-1846, 1981.

Suzuki H., K. Suzuki, and T. Sato. Dissimilarity between heat and mass transfer in a turbulent boundary layer disturbed by a cylinder. *Int. J. Heat Mass Transfer*, **31**, (2), 259-265, 1988.

Tenneks H. and J.L. Lumnly. A First Course in Turbulence. *The MIT Press*, Cambridge, Massachusetts, 1972.